# Effect of nondiagonal lowest order constrained variational effective two-body matrix elements on the binding energy of closed shell nuclei

M. Modarres* and H. Mariji
*Physics Department, University of Tehran, 1439955961 Tehran, Iran*
(Received 19 June 2012; published 30 November 2012)

The binding energies of the light, the moderate and the heavy closed shell nuclei, that is, $^{4}$He, $^{12}$C, $^{16}$O, $^{28}$Si, $^{32}$S, $^{40}$Ca, $^{56}$Ni, $^{48}$Ca, $^{90}$Zr, $^{120}$Sn, and $^{208}$Pb are calculated, using all of the channels-dependent effective two-body interactions (CDEI) matrix elements, which are generated through our lowest order constrained variational (LOCV) nuclear matter calculations with the $Av_{18}$ ($J_{\max} = 2$ and 5) phenomenological nucleon-nucleon potential. The $\mathcal{J}$-coupling scheme is applied to construct the interaction Hamiltonian matrix elements in the spherical harmonics oscillator shell model basis. In the channels with $J > J_{\max}$, the CDEI are replaced by the average effective two-body interactions. It is shown that the nondiagonal matrix elements with the $Av_{18,J_{\max}=2}$ interaction increase the binding energies of nuclei; that is, the maximum magnitude of them is about 1.49 MeV for the $^{56}$Ni nucleus. However, for the similar calculations with the $Av_{18,J_{\max}=5}$ potential, they increase the binding energies of the symmetric nuclei more than the asymmetric ones; that is, the maximum magnitude of them is about 2.74 MeV for the $^{56}$Ni nucleus. Owing to the huge computational time that is obviously needed for the calculation of the matrix elements of the heavy closed shell nuclei, their binding energies are evaluated only at their saturation points, which are available from our previous works.

DOI: 10.1103/PhysRevC.86.054324 PACS number(s): 21.60.Gx, 21.10.Dr, 27.20.+n, 27.40.+z

## I. INTRODUCTION

Recently, in a series of papers based on the local density Brueckner $\mathcal{G}$ matrix idea [1,2], the binding energies and the rms radii of the light, moderate, and heavy closed shell nuclei, that is, $^{4}$He, $^{12}$C, $^{16}$O, $^{28}$Si, $^{32}$S, $^{40}$Ca, $^{56}$Ni, $^{48}$Ca, $^{90}$Zr, $^{120}$Sn, and $^{208}$Pb [3–6], were calculated. The channel and the density-dependent effective two-body interactions (CDEIs) were generated through the lowest order constrained variational (LOCV) *asymmetrical nuclear matter* method code [7–19], at different densities, with the channel-dependent Reid types [20–22] (the Reid68, the Δ-Reid68, and the Reid68Day potentials) and the operator dependent structures [23] (the *Argonne* $Av_{18}$ potential), and bare nucleon-nucleon (NN) interactions. Then, these dependents were converted to the local one by using the local density approximation (LDA) in the harmonic oscillator shell model structure. The results, which are given in Tables I, II, and VII of Ref. [6], indicate that the LDA works quite well, and they are encouraging, both with respect to the available experimental data [24] and the different model-dependent theoretical techniques [1,25–49]. However, it was concluded that, on the average, the most of the methods give the root mean square (rms) radii roughly similar to each other and close to the experimental predictions. This was not true in the case of the binding energies, however, which shows the discrepancies between −5 and −9 MeV per nucleon, less binding. However, only the properties of nuclei with the atomic number $A \leqslant 12$ can be well described with good accuracy by the Green's function Monte Carlo (GFMC), the variational and the cluster Monte Carlo (VMC and CMC, respectively), the no-core shell model (NCSM), the correlated *hyperspherical* harmonics expansion (CHHE), and the coupled-cluster (CCM) methods by using the realistic-phenomenological NN and three nucleon (NNN) interactions [37–51]. Obviously, for the $A \geqslant 12$ nuclei, beside (i) the complication and the importance of the nuclear forces (the two- and three-body, etc., interactions), (ii) the dispersion effect (the NN intermediate states), (iii) the mean-field potential of the other nucleons on the probe nucleon (especially in the heavy nuclei), (iv) the finite size effects, as well as (v) the higher cluster terms [2,22,52], the main problem is the huge computational time. However, a few of the above complications are not necessary in the case of the infinite asymmetrical nuclear matter, that is, finite size effect, the higher cluster, etc. In several of our previous works, it has been shown that the application of the LOCV method [7–19] to nuclear matter by using the different realistic phenomenological NN potentials [2,20–23,52], gives substantially too much binding and the large saturation density with respect to the empirical one. During the last three decades, the situations have been the same for the other techniques [2,53–60] and the potentials [2,20–23,52]. However, the inclusion of the three-body force (3BF) and the Δ isobar degrees of freedom (Δ-Reid68) [2,7,8,53,54] have improved the behavior of the *Coester* line in the right direction [2,53,54]. In Refs. [61] and [62], by using the Urbana parameterized and density-dependent 3BF [63] and the cutoff-dependent N$^3$LO 2BF and N$^2$LO 3BF from the chiral perturbation field theory [64], respectively, the authors have tried to obtain the results close to the nuclear matter empirical saturation energy and density. However, beside the existence of parameters $A$ and $U$ [63] and the cutoffs Λ and $\Lambda_{3BF}$ [64], their results are not much different, for example, from our LOCV calculation with the inclusion of isobar-box-diagram [3,4,8], that is, the Δ-Reid68 realistic potential, which fits NN phase shifts. So if the uncertainties in the applications of the many-body techniques are ignored, still one can conclude that there are discrepancies between the microscopic calculations

*Corresponding author: mmodares@ut.ac.ir

 

TABLE I. The dimensions of $\mathcal{J}$ matrices of some closed shell symmetric and asymmetric nuclei and the values of their related $\mathcal{J}$'s (see the text).

| Nucleus | $^{4}$He | $^{12}$C | $^{16}$O | $^{28}$Si | $^{32}$S | $^{40}$Ca | $^{56}$Ni |
|---|---|---|---|---|---|---|---|
| $\mathcal{J}$ | 0 | 0–3 | 0–3 | 0–5 | 0–5 | 0–5 | 0–7 |
| $N \times N$ | $1 \times 1$ | $4 \times 4$ | $9 \times 9$ | $16 \times 16$ | $25 \times 25$ | $36 \times 36$ | $49 \times 49$ |
| Nucleus | $^{48}$Ca | | $^{90}$Zr | | $^{120}$Sn | | $^{208}$Pb |
| $\mathcal{J}$ | 0–7 | | 0–9 | | 0–9 | | 0–13 |
| $N \times N$ | $49 \times 49$ | | $121 \times 121$ | | $225 \times 225$ | | $484 \times 484$ |

and the empirical values of the saturation density and energy of nuclear matter at least because of the treatments of 3BF; that is, it is model dependent. However, in our future works we hope we could evaluate the effect of the 3BF directly.

For the convergence of the LOCV formalism [18,19] and the comparison of our result for nuclear matter with the other many-body techniques, see the Tables I and II of our works in Refs. [65–67]. In our recent report [68] a detail comparison has been made between the LOCV and the FHNC formalisms.

So, regarding the above discussions, it is not clear yet that the overbinding in the case of the nuclear matter and the underbinding in the case of the finite nuclei is attributable to the available phenomenological nucleon-nucleon potentials, or the application of different many-body model-dependent techniques, in which one should make several approximations (even in Refs. [3,4], the inclusion of the $\Delta$ isobar degree of freedom, which is the part of 3BF, has made the result worse).

To speed up the numerical calculations, in our pervious works on finite nuclei [3–6], an approximation was made and only the diagonal matrix elements of the LOCV-CDEI were calculated. In the present report, it is intended to calculate the whole Hamiltonian diagonal and nondiagonal matrix elements in the assumed shell model structure and perform an exact *diagonalization* procedure to find the true binding energy of the above nuclei in the framework of LDA. Then it is possible to find out the origin of above discrepancies in our previous reports [3–6]. It is worth mentioning that the digonalization of the nuclear many body Hamiltonian for various nuclei ($A \leqslant 56$) has been also preformed by using other methods such as: the similarity *renormalization* group (SRG) [69], the Faddeev random-phase approximation (FRPA) [70], the unitary model operator (UMOA) [71], and the coupled cluster (CC) [72–75] approaches. In Ref. [75] the effect of higher relative partial waves on the binding energy of $^{40}$Ca was investigated, and it is analyzed in this work.

So the paper is structured as follows. In Sec. II, the shell model structure for each nucleus, the method that is applied to calculate the matrix elements of specific nucleus Hamiltonian, and the corresponding diagonalization procedure, are briefly explained. Finally, the results, discussion, and conclusion are presented in the Sec. III.

## II. THE CALCULATION OF NONDIAGONAL MATRIX ELEMENTS OF THE NUCLEUS HAMILTONIAN

As before [3–6], the harmonic oscillator shell model basis is chosen and the nucleon configurations of the different symmetric light and moderate closed shell nuclei are assumed as

$$^{4}\mathrm{He} : \left[\left(0s_{\frac{1}{2}}\right)^{4}\right],\ ^{12}\mathrm{C} : \left[^{4}\mathrm{He} + \left(0p_{\frac{3}{2}}\right)^{8}\right],\ ^{16}\mathrm{O} : \left[^{12}\mathrm{C} + \left(0p_{\frac{1}{2}}\right)^{4}\right],\ ^{28}\mathrm{Si} : \left[^{16}\mathrm{O} + \left(0d_{\frac{5}{2}}\right)^{12}\right], \tag{1}$$

and (note that in this work, the principle quantum numbers $n_i$ are started from zero rather one)

$$^{32}\mathrm{S} : \left[^{28}\mathrm{Si} + \left(1s_{\frac{1}{2}}\right)^{4}\right],\ ^{40}\mathrm{Ca} : \left[^{32}\mathrm{S} + \left(0d_{\frac{3}{2}}\right)^{8}\right],\ ^{56}\mathrm{Ni} : \left[^{40}\mathrm{Ca} + \left(0f_{\frac{7}{2}}\right)^{16}\right], \tag{2}$$

respectively. Also, for the asymmetric heavy closed shell nuclei, the following shell model configurations are used [4,6]:

$$\begin{aligned}
&^{48}\mathrm{Ca} : {}^{40}\mathrm{Ca} + \left[\left(0f_{\frac{7}{2}}\right)^{8}\right]_{n},\ ^{90}\mathrm{Zr} : {}^{40}\mathrm{Ca} + \left[(0f)^{28}(1p)^{12}\right] + \left[\left(0g_{\frac{9}{2}}\right)^{10}\right]_{n},\\
&^{120}\mathrm{Sn} : {}^{40}\mathrm{Ca} + \left[(0f)^{28}(1p)^{12}\left(0g_{\frac{9}{2}}\right)^{20}\right] + \left[\left(0g_{\frac{7}{2}}\right)^{8}(1d)^{10}(2s)^{2}\right]_{n},\\
&^{208}\mathrm{Pb} : {}^{40}\mathrm{Ca} + \left[(0f)^{28}(1p)^{12}(0g)^{36}(1d)^{20}(2s)^{4}\left(0h_{\frac{11}{2}}\right)^{24}\right] + \left[\left(0h_{\frac{9}{2}}\right)^{10}(1f)^{14}(2p)^{6}\left(0i_{\frac{13}{2}}\right)^{14}\right]_{n}.
\end{aligned} \tag{3}$$

As was already mentioned [3–6], the single nucleon states, $\phi_i$, are defined in terms of the harmonic oscillator (HOS) wave functions, and the oscillator parameter $\gamma = \sqrt{\frac{\hbar\omega}{M}}$ is assumed as the variational parameter to fix the rms radius of specific nucleus, where $\hbar\omega$ is the familiar quantum energy of our HOS basis. Assuming the origin of our coordinate to be fixed at each nucleus center of mass, then the intrinsic Hamiltonian is given by

$$\mathcal{H}_0 = \{\mathcal{H}\} - \frac{\mathbf{P}^2}{\mathcal{M}}, \tag{4}$$

TABLE II. The matrix elements of $\mathcal{T}_2$ and $\mathcal{V}_2$ for $^{208}$Pb nucleus by using all of the CDEI, for the $Av_{18}$ interaction with $J_{\max} = 2$, in terms of $\mathcal{J}$.

| $\mathcal{J}$ | $T=0,\ M_T=0$ | | $T=1,\ M_T=-1$ | | $T=1,\ M_T=0$ | | $T=1,\ M_T=1$ | |
|---|---|---|---|---|---|---|---|---|
| | $\frac{\mathcal{T}_2}{A}$ | $\frac{\mathcal{V}_2}{A}$ | $\frac{\mathcal{T}_2}{A}$ | $\frac{\mathcal{V}_2}{A}$ | $\frac{\mathcal{T}_2}{A}$ | $\frac{\mathcal{V}_2}{A}$ | $\frac{\mathcal{T}_2}{A}$ | $\frac{\mathcal{V}_2}{A}$ |
| 0 | 0.193 | −0.314 | 0.181 | −0.428 | 0.135 | −0.391 | 0.124 | −0.326 |
| 1 | 2.051 | −3.061 | 0.490 | −0.967 | 0.381 | −0.820 | 0.301 | −0.642 |
| 2 | 1.756 | −4.319 | 0.604 | −2.078 | 0.469 | −1.762 | 0.154 | −0.584 |
| 3 | 1.853 | −4.794 | 0.656 | −2.282 | 0.477 | −1.828 | 0.369 | −1.370 |
| 4 | 1.786 | −4.688 | 0.627 | −2.257 | 0.432 | −1.703 | 0.105 | −0.526 |
| 5 | 1.549 | −4.180 | 0.339 | −1.164 | 0.367 | −1.471 | 0.095 | −0.319 |
| 6 | 1.294 | −3.527 | 0.433 | −1.576 | 0.280 | −1.137 | 0.149 | −0.493 |
| 7 | 0.142 | −0.403 | 0.191 | −0.624 | 0.175 | −0.637 | 0.136 | −0.546 |
| 8 | 0.269 | −0.699 | 0.064 | −0.228 | 0.124 | −0.571 | 0.080 | −0.341 |
| 9 | 0.366 | −1.067 | 0.050 | −0.148 | 0.080 | −0.360 | 0.042 | −0.167 |
| 10 | 0.302 | −0.893 | 0.021 | −0.059 | 0.042 | −0.175 | 0.005 | −0.015 |
| 11 | 0.151 | −0.452 | 0.047 | −0.181 | 0.005 | −0.016 | — | — |
| 12 | 0.084 | −0.250 | 0.006 | −0.014 | 0.000 | −0.001 | — | — |
| 13 | 0.000 | −0.000 | 0.000 | −0.000 | 0.000 | −0.000 | — | — |

where $\mathbf{P} = \sum_i \mathbf{p_i}$ and $\mathcal{M} = AM$ are the nucleus total linear momentum and its mass, respectively. Thus, the total ground-state binding energy of a nucleus can be obtained through the expectation value of the above Hamiltonian ($\mathcal{H}_0$):

$$E^{\rm BE}_{\rm Total} = \langle \mathcal{H}_0 \rangle = \left\{ \left[ \sum_i \langle i,\gamma | \frac{p^2}{2M} | i,\gamma \rangle \right] + \overline{\left[ \frac{1}{4} \sum_{ijkl} \langle ij,\gamma | \mathcal{V}_{\rm eff}(12,\rho) | kl,\gamma \rangle_a \right]} \right\} - T^A_{\rm c.m.}, \quad (5)$$

in the HOS basis, where the Dirac *ket* $|i;\gamma\rangle$ stands for $|n_i, l_i, s_i, \tau_i, m_{\tau i};\gamma\rangle$, that is, the principle quantum number, the angular momentum, the spin, the isospin, and the isospin projection parts of the single particle states, respectively. It is well known that in the nuclei, $\mathbf{l}_i + \mathbf{s}_i$ should be replaced by the good operator $\mathbf{j}_i$ because of the spin-orbit interactions. The kinetic energy related to each nucleus *center-of-mass* motion is

$$T^A_{\rm c.m.} = \left\langle \frac{\mathbf{P}^2}{\mathcal{M}} \right\rangle = \frac{3}{4}\hbar\omega.$$

The matrix elements of *one-body*, that is, $\frac{p^2}{2M}$, kinetic energy per nucleon has the familiar form of

$$T_1 = \frac{1}{A}\sum_i^A \langle i,\gamma | \frac{p^2}{2M} | i,\gamma \rangle = \frac{1}{2A}\sum_{i=1}^A \left(2n_i + l_i + \frac{3}{2}\right)\hbar\omega, \quad (6)$$

and it is diagonal in the HO basis. The nonlocal two-body effective interaction operator, $\mathcal{V}_{\rm eff}(1,2)$, has the following form [53]:

$$\mathcal{V}_{\rm eff}(1,2) = \{\mathcal{T}_2\} + \{\mathcal{V}_2\} = \left\{ \frac{-\hbar^2}{2m} \left[ F(1,2), \left[ \nabla^2_{12}, F(1,2) \right] \right] \right\} + \{F(1,2)V(12)F(1,2)\}, \quad (7)$$

where $F(1,2)$ and $V(12)$ are the two-body correlation functions and the phenomenological NN potentials, respectively. We should diagonal the matrix with elements

$$\left[ \tfrac{1}{4} \langle ij,\gamma | \mathcal{V}_{\rm eff}(12,\rho) | kl,\gamma \rangle_a \right], \quad (8)$$

where $i$, $j$, $k$, and $l$ run over the model space defined in Eqs. (1), (2), and (3) for each nucleus with the atomic number $A$. By the term

$$\overline{[\mathcal{V}_{\rm eff}]} = \overline{\left[ \frac{1}{4} \sum_{ijkl} \langle ij,\gamma | \mathcal{V}_{\rm eff}(12,\rho) | kl,\gamma \rangle_a \right]} \quad (9)$$

in Eq. (5), we mean the sum of diagonal elements of two-body effective interaction matrix (8), after diagonalization (see below for definition of its matrix elements). We choose the modern phenomenological Argonne $Av_{18}$ interaction as the bare NN potential [23]. To take into account the nondiagonal contributions of the two-body effective interactions to the binding energies of the closed shell nuclei, unlike our previous works [3–6], the related matrices should be constructed by using the following interaction elements:

$$\xi_I^{\mathcal{J}T}(\eta_1\eta_2, \eta_1'\eta_2') = \langle \eta_1'\eta_2'; \mathcal{J}T | \mathcal{V}_{\rm eff}(1,2) | \eta_1\eta_2; \mathcal{J}T \rangle \quad (10)$$

for the symmetric nuclei and

$$\xi_I^{\mathcal{J}TM_T}(\eta_1\eta_2, \eta_1'\eta_2') = \langle \eta_1'\eta_2'; \mathcal{J}TM_T | \mathcal{V}_{\rm eff}(1,2) | \eta_1\eta_2; \mathcal{J}TM_T \rangle \quad (11)$$

for the asymmetric nuclei. In the above equations $\mathcal{J}$, $T$, and $M_T$ are the total angular momentum, $\overrightarrow{\mathcal{J}} = \overrightarrow{j_1} + \overrightarrow{j_2}$, the total isospin and the total isospin projection of the two nucleons, respectively, and the quantum number $\eta_i$ stands for the single nucleon quantum numbers $n_i, l_i$, and $j_i$. Now, in the $\mathcal{J}$-coupled scheme, the foregoing interaction matrix elements can be

written as follows [76,77]:

$$\xi_I^{\mathcal{J}TM_T}(\eta_1\eta_2,\eta_1'\eta_2') = \sum_{nLN\mathcal{L},\lambda}\sum_{n'L'N'\mathcal{L}',\lambda'}\sum_{JSm_{\tau_1}m_{\tau_2}}\sqrt{[j_1][j_2][j_1'][j_2']}[\mathcal{J}][J][S][\lambda][\lambda'](-1)^{\lambda+\lambda'}[1-(-1)^{L+S+T}](\tau_1,\tau_2,m_{\tau_1},m_{\tau_2}|TM_T)$$
$$\times\langle n_1l_1n_2l_2;\lambda|nLN\mathcal{L};\lambda\rangle\langle n'_1l'_1n'_2l'_2;\lambda'|n'L'N'\mathcal{L}';\lambda'\rangle\begin{Bmatrix}\mathcal{L}&L&J\\S&\mathcal{J}&\lambda\end{Bmatrix}_{6j}\begin{Bmatrix}\mathcal{L}'&L'&J\\S&\mathcal{J}&\lambda'\end{Bmatrix}_{6j}\begin{Bmatrix}l_1&\frac{1}{2}&j_1\\l_2&\frac{1}{2}&j_2\\\lambda&S&J\end{Bmatrix}_{9j}\begin{Bmatrix}l'_1&\frac{1}{2}&j'_1\\l'_2&\frac{1}{2}&j'_2\\\lambda'&S&J\end{Bmatrix}_{9j}$$
$$\times\langle n'L'JST,M_T,N'\mathcal{L}'|\mathcal{V}_{eff}^{LJSTM_T}(|\overrightarrow{r}_{12}|,\rho(|\overrightarrow{R}_{12}|))|nLJST,M_T,N\mathcal{L}\rangle, \quad (12)$$

where $[j_1]=2j_1+1$, etc., $\langle n_1l_1n_2l_2;\lambda|nLN\mathcal{L};\lambda\rangle$, etc., are the *Brody-Moshinsky* brackets [78] and $\overrightarrow{r}_{12}=\overrightarrow{r}_1-\overrightarrow{r}_2$ and $\overrightarrow{R}_{12}=\frac{\overrightarrow{r}_1+\overrightarrow{r}_2}{2}$. The parameters and the quantum numbers in the above equations are similar to those given in Refs. [3–6]. Here, again, the LDA approach [3–6] is used for $\rho(|\overrightarrow{R}_{12}|)$. For the symmetric nuclei, it is possible to remove the *Clebsch-Gordon* coefficients $(\tau_1,\tau_2,m_{\tau_1},m_{\tau_2}|TM_T)$ in the above equation and replace it with $[T]$. It should be pointed out that, in general, $\mathcal{V}_{\rm eff}^{LSJTM_T}(\overrightarrow{r}_{12},\rho(|\overrightarrow{R}_{12}|))$ depend on the asymmetric parameter, $\Re=\frac{\rho_p}{\rho_n}$, where $\rho_{p(n)}$ is the single-particle density of protons (neutrons) [4,6]. To construct the interaction matrix by using the interaction matrix elements $\xi_I^{\mathcal{J}TM_T}$, it should be mentioned that there are two $\mathcal{J}$ block matrices corresponding to $T=0$ (one block) and $T=1$ (one block which contains three sub-blocks for different $M_T$ values). So, four $\mathcal{J}$ block matrices could be constructed by means of $\xi_I^{\mathcal{J}TM_T}$ elements, corresponding to $T=0$, $M_T=0$ and $T=1$, $M_T=-1,0,1$. Now, for a symmetric (asymmetric) nucleus, a $N\times N$ $\mathcal{J}$ matrices can be built by the elements of $\xi_I^{\mathcal{J}T(M_T)}$. To write a computing program, it is useful to arrange the matrix elements as the nucleons occupy the energy levels in the corresponding shell configurations. In this view, the quantum numbers are sorted to get the row (column) indices, $i(j)$, as follows:

$$i = n_1(m_{l1}m_{j_1}m_{n2}m_{l2}m_{j_2})+l_1(m_{j_1}m_{n2}m_{l2}m_{j_2}) + j_1(m_{n2}m_{l2}m_{j_2})+n_2(m_{l2}m_{j_2})+l_2(m_{j_2})+j_2+\tfrac{1}{2}. \quad (13)$$

The numbers $m_\eta$ are the maximum possible values that can be taken by $\eta$, and as before, $\eta$ implies $n_i$, $l_i$, $j_i$ which corresponds to each occupied energy level in the shell model. Because $j_i$ has a half-odd magnitude, it is useful to add $\frac{1}{2}$ in the above equation. To clarify, consider the $^{40}$Ca nucleus as an example. In this nucleus, the values of $\{n_i\}$, $\{l_i\}$, and $\{j_i\}$ are $\{0,1\}$, $\{0,1,2\}$, and $\{\frac{1}{2},\frac{3}{2},\frac{5}{2}\}$, respectively. Thus, from Eq. (13), $m_n=2$, $m_l=3$, and $m_j=3$. In this way, one can trace the related matrix elements without confusing. Now, the $\mathcal{J}$-matrix elements can be constructed as

$$\begin{aligned}\xi_{11}^{\mathcal{J}T}&=\langle 0s_{\frac{1}{2}},0s_{\frac{1}{2}}|\xi_I^{\mathcal{J}T}|0s_{\frac{1}{2}},0s_{\frac{1}{2}}\rangle,\\ \xi_{12}^{\mathcal{J}T}&=\langle 0s_{\frac{1}{2}},0s_{\frac{1}{2}}|\xi_I^{\mathcal{J}T}|0s_{\frac{1}{2}},0p_{\frac{3}{2}}\rangle,\\ \ldots,\xi_{1,36}^{\mathcal{J}T}&=\langle 0s_{\frac{1}{2}},0s_{\frac{1}{2}}|\xi_I^{\mathcal{J}T}|0d_{\frac{3}{2}},0d_{\frac{3}{2}}\rangle,\end{aligned} \quad (14)$$

$$\begin{aligned}\xi_{21}^{\mathcal{J}T}&=\langle 0s_{\frac{1}{2}},0p_{\frac{3}{2}}|\xi_I^{\mathcal{J}T}|0s_{\frac{1}{2}},0s_{\frac{1}{2}}\rangle,\\ \xi_{22}^{\mathcal{J}T}&=\langle 0s_{\frac{1}{2}},0p_{\frac{3}{2}}|\xi_I^{\mathcal{J}T}|0s_{\frac{1}{2}},0p_{\frac{3}{2}}\rangle,\\ \ldots,\xi_{2,36}^{\mathcal{J}T}&=\langle 0s_{\frac{1}{2}},0p_{\frac{3}{2}}|\xi_I^{\mathcal{J}T}|0d_{\frac{3}{2}},0d_{\frac{3}{2}}\rangle,\end{aligned} \quad (15)$$

etc., and finally,

$$\begin{aligned}\xi_{36,1}^{\mathcal{J}T}&=\langle 0d_{\frac{3}{2}},0d_{\frac{3}{2}}|\xi_I^{\mathcal{J}T}|0s_{\frac{1}{2}},0s_{\frac{1}{2}}\rangle,\\ \xi_{36,2}^{\mathcal{J}T}&=\langle 0d_{\frac{3}{2}},0d_{\frac{3}{2}}|\xi_I^{\mathcal{J}T}|0s_{\frac{1}{2}},0p_{\frac{3}{2}}\rangle,\\ \ldots,\xi_{36,36}^{\mathcal{J}T}&=\langle 0d_{\frac{3}{2}},0d_{\frac{3}{2}}|\xi_I^{\mathcal{J}T}|0d_{\frac{3}{2}},0d_{\frac{3}{2}}\rangle.\end{aligned} \quad (16)$$

There are six $\mathcal{J}$ matrices according to the different values of $\mathcal{J}$ for $^{40}$Ca; that is, $\mathcal{J}=0$–5. Therefore, there exits totally 12 $\mathcal{J}$ matrices with $36\times36$ dimension. Table I, shows the matrix dimensions of the above-mentioned closed shell symmetric and asymmetric nuclei as well as the values of their corresponding $\mathcal{J}$'s. Of course, Table I just shows the maximum dimensions of $\mathcal{J}$ matrices of asymmetric nuclei. After constructing the $\mathcal{J}$ matrices, they should be diagonalized by using an appropriate diagonalization code. In this work the EISPACK [79] code (which was available for us) is used for this purpose. Thus, the contributions of the two-body interactions in the ground state of the closed shell nuclei can be obtained from the sum of these interaction $\mathcal{J}$ matrices eigenvalues. The calculations are performed by using the $Av_{18,J_{\max}=2}$ and $Av_{18,J_{\max}=5}$ interactions, with inclusion of the Coulomb potential, for the symmetric and the asymmetric nuclei. Note that, because we are working in the $\mathcal{J}$-coupled basis in which the coupled angular momentum has a definite value, it is more beneficial to use $\mathcal{J}$ scheme rather than $\mathcal{M}$ scheme, to construct the interaction matrices. Although $\mathcal{M}$ scheme consumes less computing time than $\mathcal{J}$ scheme, it is not suitable for the matrix elements which are formulated in the present formalism.

However, because, especially, the dimensions of $\mathcal{J}$ matrices of the heavy closed nuclei are very large, the huge computing times are needed. For example, the calculation of $484\times484$ elements of $\mathcal{J}$ matrix of $^{208}$Pb, with $\mathcal{J}\leqslant7$, takes approximately about 600 h of CPU time by means of a PC (Pentium 4; 2.8 GHz; 1-MB cache; 2 GB RAM) with LINUX operating system (CENTOS 5.1). Of course, this time reduces to about 100 h for $\mathcal{J}$ matrices of $^{208}$Pb, with $7\leqslant\mathcal{J}<13$ [note that

TABLE III. As the Table I but for $J_{\max} = 5$.

| $\mathcal{J}$ | $T = 0,\ M_T = 0$ | | $T = 1,\ M_T = -1$ | | $T = 1,\ M_T = 0$ | | $T = 1,\ M_T = 1$ | |
|---|---|---|---|---|---|---|---|---|
| | $\frac{\mathcal{T}_2}{A}$ | $\frac{\mathcal{V}_2}{A}$ | $\frac{\mathcal{T}_2}{A}$ | $\frac{\mathcal{V}_2}{A}$ | $\frac{\mathcal{T}_2}{A}$ | $\frac{\mathcal{V}_2}{A}$ | $\frac{\mathcal{T}_2}{A}$ | $\frac{\mathcal{V}_2}{A}$ |
| 0 | 0.121 | −0.266 | 0.143 | −0.337 | 0.106 | −0.307 | 0.096 | −0.253 |
| 1 | 1.150 | −2.318 | 0.409 | −0.806 | 0.318 | −0.683 | 0.251 | −0.541 |
| 2 | 1.489 | −3.677 | 0.526 | −1.833 | 0.385 | −1.462 | 0.312 | −1.168 |
| 3 | 1.571 | −3.828 | 0.534 | −1.788 | 0.365 | −1.214 | 0.301 | −1.092 |
| 4 | 1.507 | −3.898 | 0.506 | −1.831 | 0.350 | −1.390 | 0.267 | −1.054 |
| 5 | 1.302 | −3.400 | 0.429 | −1.548 | 0.187 | −0.736 | 0.209 | −0.808 |
| 6 | 0.698 | −1.806 | 0.353 | −1.320 | 0.225 | −0.917 | 0.159 | −0.649 |
| 7 | 0.821 | −2.271 | 0.263 | −0.995 | 0.095 | −0.327 | 0.108 | −0.451 |
| 8 | 0.608 | −1.715 | 0.191 | −0.763 | 0.110 | −0.481 | 0.064 | −0.138 |
| 9 | 0.395 | −1.153 | 0.126 | −0.517 | 0.063 | −0.297 | 0.034 | −0.015 |
| 10 | 0.250 | −0.747 | 0.072 | −0.312 | 0.032 | −0.142 | 0.004 | −0.012 |
| 11 | 0.125 | −0.378 | 0.037 | −0.152 | 0.004 | −0.012 | — | — |
| 12 | 0.069 | −0.207 | 0.004 | −0.011 | 0.000 | −0.000 | — | — |
| 13 | 0.000 | −0.000 | 0.000 | −0.000 | 0.000 | −0.000 | — | — |

this time is required (1) mainly for the calculation of the matrix element, for example, calculation of each matrix element for the $^{208}$Pb nucleus takes at least between 2 and 5 min and (2) for the diagonalization].

## III. RESULTS, DISCUSSIONS, AND CONCLUSIONS

Tables II and III, show the break down of diagonalized matrix elements of the two-body kinetics ($\mathcal{T}_2$) and potentials ($\mathcal{V}_2$) energies per nucleon for the $^{208}$Pb nucleus in terms of $\mathcal{J}$, $T$, and $M_T$. They are obtained by using all of the matrix elements of the CDEI for the $Av_{18}$ interaction with $J_{\max} = 2$ and 5, respectively. In general, for the different values of the total isospin $T$, as $\mathcal{J}$ increases, the absolute values of $\mathcal{T}_2$ and $\mathcal{V}_2$ also increase and then for $4 \leqslant \mathcal{J} \leqslant 6$ they start to decrease. As one should expect, the singlet isospin components; that is, $T = 0,\ M_T = 0$ has larger two-body kinetic and lower two-body potential energies. However, for the triplet case, $T = 1$, again it is observed that while $\mathcal{T}_2$ decreases, the two-body potential energy increases when the isospin projection changes from $M_T = -1$ to 0 or 1. By changing $J_{\max}$ from 2 to 5, in general, all of the matrix element absolute values decease. So in the present calculation, and similar to our previous report [6], the inclusion of the higher channels in the potential, force the binding energy to decrease.

The differences of variational binding energies per nucleon (MeV) of the light and the moderate symmetric closed shell nuclei which are obtained by using all of the matrix elements of CDEI (this work) and the diagonal ones (the previous work) [5], with the $Av_{18}$ interaction up to $J_{\max} = 2$ and $J_{\max} = 5$ are given in Tables IV and V, respectively. In these tables, the first column shows the nucleus types and the second one gives the difference of oscillation parameters, $\gamma$, between the two saturation points, that is, with and without inclusion of the nondiagonal effects [5]. The six other columns again show the differences between two latter cases for the single-particle kinetic energy, the two-body kinetic energy, the two-body potential energy, the Coulomb energy, the binding energy, and the rms radius of the light and the moderate closed shell symmetric nuclei. For the case of $J_{\max} = 2$, in Table IV, generally for most of the nuclei, the rms radii ($\gamma$) do not change, which shows that the diagonalization has not affected the rms radii. Only in case of the $^{12}$C and $^{56}$Ni nuclei are the rms radii decreased. A similar situation is held for the binding energies, in which there are about 1.08- and 1.49-MeV increase in the binding energies of the $^{28}$Si and $^{56}$Ni nuclei, respectively. Looking at Table V, that is, the $J_{\max} = 5$ case, one notices that while the rms radii do not change at all, which is in contrast to the $J_{\max} = 2$ case, the difference in the binding energies

TABLE IV. The difference of the variational binding energies per nucleon (MeV) and the rms radii (fm) of the light and the moderate symmetric closed shell nuclei obtained by using all of the matrix elements of CDEI (present work) and just by using the diagonal ones from Ref. [5], with the $Av_{18}$ interaction up to the $J_{\max} = 2$. See the text for explanations about the different columns.

| Nucleus | $\Delta\gamma$ | $\frac{\Delta T_1}{A}$ | $\frac{\Delta \mathcal{T}_2}{A}$ | $\frac{\Delta \mathcal{V}_2}{A}$ | $\frac{\Delta V_c}{A}$ | $\frac{\Delta \mathrm{BE_c}}{A}$ | $\Delta r_{\mathrm{rms}}$ |
|---|---|---|---|---|---|---|---|
| $^{12}$C | 0.02 | 1.07 | 1.1 | −2.66 | −0.02 | −0.50 | −0.07 |
| $^{16}$O | 0.00 | 0.00 | −0.02 | 0.11 | −0.04 | 0.05 | 0.00 |
| $^{28}$Si | 0.01 | 0.7 | 0.82 | −2.42 | −0.19 | −1.08 | −0.05 |
| $^{32}$S | 0.00 | 0.00 | 0.25 | −0.32 | −0.17 | −0.24 | 0.00 |
| $^{40}$Ca | −0.01 | −0.72 | −0.59 | 1.48 | −0.31 | −0.13 | 0.05 |
| $^{56}$Ni | 0.02 | 1.66 | 1.65 | −4.35 | −0.45 | −1.49 | −0.10 |

TABLE V. The same as Table IV but for $Av_{18}$ interaction with $J_{\max} = 5$. See the text for explanations about the different columns.

| Nucleus | $\Delta\gamma$ | $\frac{\Delta T_1}{A}$ | $\frac{\Delta T_2}{A}$ | $\frac{\Delta V_2}{A}$ | $\frac{\Delta V_c}{A}$ | $\frac{\Delta \mathrm{BE}_c}{A}$ | $\Delta r_{\mathrm{rms}}$ |
|---|---|---|---|---|---|---|---|
| $^{12}$C | 0.01 | 0.53 | 1.64 | −3.96 | −0.03 | −1.82 | −0.03 |
| $^{16}$O | 0.00 | 0.00 | 1.04 | −2.32 | −0.04 | −1.32 | 0.00 |
| $^{28}$Si | 0.00 | 0.00 | 1.48 | −3.68 | −0.21 | −2.41 | 0.00 |
| $^{32}$S | −0.01 | −0.70 | 0.84 | −1.63 | −0.21 | −1.68 | 0.04 |
| $^{40}$Ca | −0.01 | −0.72 | 0.62 | −1.15 | −0.31 | −1.56 | 0.05 |
| $^{56}$Ni | 0.00 | 0.00 | 1.51 | −3.71 | −0.55 | −2.74 | 0.00 |

becomes much larger with respect to the nondiagonalized calculations.

The effect of nondiagonal matrix elements on the binding energy can be investigated by comparing these contributions, that is, Tables IV and V with those presented in our previous works [5,6]. The nondiagonal matrix elements lead to shift the saturation binding energies of the light and the moderate closed shell nuclei to the lower ones. This behavior is demonstrated in Fig. 1, in which the dash (full) curves are from our previous (present) work. While, there are obviously no changes in the ground-state energy of $^4$He nucleus, the diagonalization procedures increase the binding energies of the light and the moderate nuclei with respect to the nondiagonalization case [5]. The shifts are larger near the saturation points. However, still the present results are far from the experimental data, that is, the stars in the Fig. 1, but one hopes that working in the larger configuration space, for example including the $1s0d$ shell in $^{16}$O, etc., may shift the saturation binding energy to the lower one. Evidence of this argument can be observed in the heavy nuclei. However, we could not estimate the effect of the nondiagonal matrix elements on the saturation points of the heavy nuclei because of the computing time problems. So we force to calculate their binding energies only near the nondiagonalized [5] saturation points. So, the Tables VI ($Av_{18}$ with $J_{\max} = 2$) and VII ($Av_{18}$ with $J_{\max} = 5$) are the same as two above latter tables and show the differences between the results of present and our previous works [6] for the asymmetric closed shell nuclei. Because (1) for the symmetric nuclei we found that the rms radii ($\gamma$) do not change and (2) as it was pointed out before, the numerical calculation for the heavy closed shell nuclei need an enormous computational time, so the calculations are performed only at the saturation points obtained from nondiagonalized calculations [6]. It is interesting that while in case of $J_{\max} = 2$, the binding energy increases for the $^{48}$Ca, $^{90}$Zr, and $^{120}$Sn nuclei it decreases for $^{208}$Pb nucleus. For example, the diagonalization procedure changes the binding energy of $^{208}$Pb nucleus from −9.22 to −7.92 MeV, which approaches the experimental predication of −7.87 MeV.

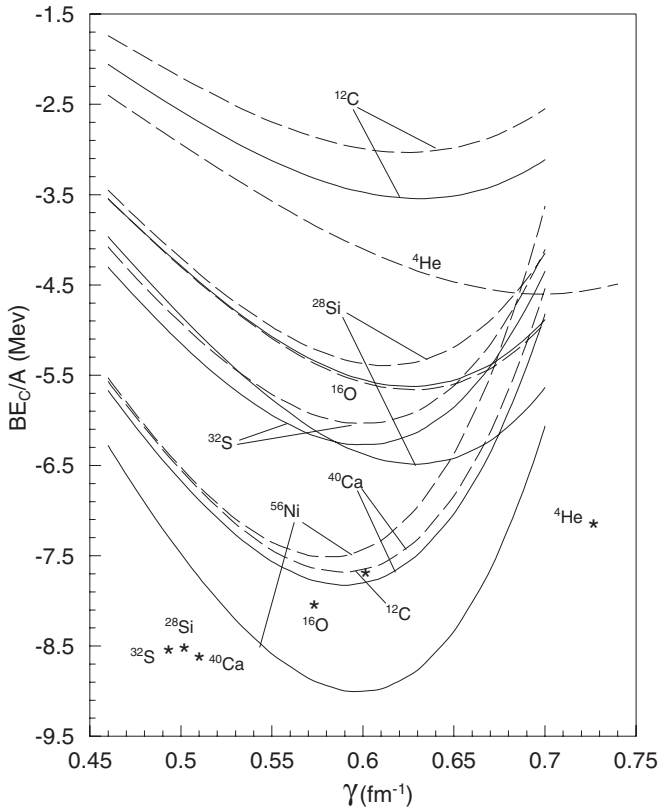


FIG. 1. The saturation curve of the light and the moderate closed shell nuclei. Solid curves, present work; dashed curves, from Ref. [5]).

Figure 2 of Ref. [75] shows that by changing $J_{\max}$ from 4 (5) to 5 (10) the variation of the binding energy of $^{40}$Ca is about 0.3 (0.15) MeV per nucleon. However, in the Tables I and III of Ref. [5] the difference between $J_{\max} = 2$ and $J_{\max} = 5$ is about 0.32 MeV per nucleon. So we do not expect to observe the sizable changes by performing calculation up to $J_{\max} = 10$, which needs much more computer time. As we pointed out before, the LOCV calculation for nuclear matter with the phenomenological potentials such as $Av_{18}$ agrees well with FHNC calculation (see our recent work in Ref. [68]) and it is reasonably convergent [18,19]. So the results of our diagolaization in this work shows the accuracy of our previous works in which only the diagonal matrix elements have been taken into the account. However, in our future works we will try to investigate the importance of the higher relative partial-wave

TABLE VI. The same as the Table IV but for asymmetric nuclei.

| Nucleus | $\gamma$ | $\frac{\Delta T_2}{A}$ | $\frac{\Delta V_2}{A}$ | $\frac{\Delta V_c}{A}$ | $\frac{\Delta \mathrm{BE}_c}{A}$ |
|---|---|---|---|---|---|
| $^{48}$Ca | 0.59 | 0.10 | −0.49 | −0.24 | −0.64 |
| $^{90}$Zr | 0.54 | 0.13 | −0.37 | −0.57 | −0.80 |
| $^{120}$Sn | 0.52 | 0.14 | −0.31 | −0.92 | −1.09 |
| $^{208}$Pb | 0.49 | 0.15 | 2.81 | −1.66 | 1.30 |

TABLE VII. The same as the Table V but for asymmetric nuclei.

| Nucleus | $\gamma$ | $\frac{\Delta T_2}{A}$ | $\frac{\Delta V_2}{A}$ | $\frac{\Delta V_c}{A}$ | $\frac{\Delta \mathrm{BE}_c}{A}$ |
|---|---|---|---|---|---|
| $^{48}$Ca | 0.59 | 0.04 | −0.24 | −0.24 | −0.44 |
| $^{90}$Zr | 0.54 | 0.05 | −0.11 | −0.57 | −0.63 |
| $^{120}$Sn | 0.52 | −0.67 | 1.16 | −0.92 | −0.43 |
| $^{208}$Pb | 0.49 | −0.60 | 2.34 | −1.66 | 0.09 |

contribution as well the effect of uncertainty in our LOCV nuclear matter calculation.

In conclusion, the binding energies of the light, the moderate, and the heavy closed shell nuclei, that is, $^{4}$He, $^{12}$C, $^{16}$O, $^{28}$Si, $^{32}$S, $^{40}$Ca, $^{56}$Ni, $^{48}$Ca, $^{90}$Zr, $^{120}$Sn, and $^{208}$Pb were calculated, by using all of the channel-dependent effective two-body interactions matrix elements which could be calculated by performing the LOCV nuclear matter calculations with the $Av_{18}$ phenomenological NN potential for different $J_{\max} = 2$ and 5. Rather than the $\mathcal{M}$-coupling scheme the $\mathcal{J}$-coupling scheme was applied to construct the interaction Hamiltonian matrices in the spherical harmonics oscillator basis shell structure. The channel-dependent effective two-body interactions were replaced with the average effective interactions for the interaction channels with $J > J_{\max}$. It was shown that the nondiagonal matrix elements with $Av_{18,J_{\max}=2}$ interactions increase the binding energy of nuclei; that is, the maximum magnitude of them was about 1.49 MeV for the $^{56}$Ni nucleus. However, similar calculations with $Av_{18,J_{\max}=5}$ increased the binding energy of the symmetric nuclei more than the asymmetric ones; that is, the maximum magnitude of them was about 2.74 MeV for the $^{56}$Ni nucleus. Owing to the huge computational time for the heavy nuclei, the binding energies were calculated only at their saturation points which were available from our previous works. The EISPACK code was used for the above diagonalization procedure of our interaction Hamiltonian matrices. Finally it is concluded that working in the larger configuration shell model space and with inclusion of nondiagonal matrix elements as well as the effects of the higher partial waves, that is, $J_{\max} \geqslant 5$, and 3BF it could be possible to remove the discrepancies between the theoretical calculations and the experimental predications. We also hope in our future works to find out about the effects of the LDA, the harmonic oscillator approximation, and the method of diagonalization procedures on the results presented here.

## ACKNOWLEDGMENTS

We would like to thank the Research Council of University of Tehran and Institute for Research and Planning in Higher Education for the grants provided for us.

[1] J. W. Negele, Phys. Rev. C **1**, 1260 (1970).
[2] B. D. Day, Rev. Mod. Phys. **50**, 495 (1978).
[3] M. Modarres and N. Rasekhinejad, Phys. Rev. C **72**, 014301 (2005).
[4] M. Modarres and N. Rasekhinejad, Phys. Rev. C **72**, 064306 (2005).
[5] M. Modarres, N. Rasekhinejad, and H. Mariji, J. Mod. Phys. E **20**, 679 (2011).
[6] M. Modarres, H. Mariji, and N. Rasekhinejad, Nucl. Phys. A **859**, 16 (2011).
[7] J. C. Owen, R. F. Bishop, and J. M. Irvine, Ann. Phys. (NY) **102**, 170 (1976).
[8] M. Modarres and J. M. Irvine, J. Phys. G **5**, 511 (1979).
[9] M. Modarres and G. H. Bordbar, Phys. Rev. C **58**, 2781 (1998).
[10] M. Modarres, J. Phys. G **19**, 1349 (1993).
[11] M. Modarres and H. R. Moshfegh, Phys. Rev. C **62**, 044308 (2000).
[12] G. H. Bordbar and M. Modarres, J. Phys. G: Nucl. Part. Phys. **23**, 1631 (1997).
[13] G. H. Bordbar and M. Modarres, Phys. Rev. C **57**, 714 (1998).
[14] M. Modarres and J. M. Irvine, J. Phys. G: Nucl. Phys. **5**, 7 (1979).
[15] H. R. Moshfegh and M. Modarres, J. Phys. G **24**, 821 (1998).
[16] M. Modarres and H. R. Moshfegh, Prog. Theor. Phys. **112**, 21 (2004).
[17] H. R. Moshfegh and M. Modarres, Nucl. Phys. A **759**, 79 (2005).
[18] M. Modarres, A. Rajabi, and H. R. Moshfegh, Phys. Rev. C **76**, 064311 (2007).
[19] M. Modarres, H. R. Moshfegh, and K. Fallahi, Eur. Phys. J. B **36**, 485 (2003).
[20] R. V. Reid, Ann. Phys. (NY) **50**, 411 (1969).
[21] A. M. Green, J. A. Niskanan, and M. E. Sainio, J. Phys. G **4**, 1085 (1978).
[22] B. D. Day, Phys. Rev. C **24**, 1203 (1981).
[23] R. B. Wiringa, V. G. J. Stoks, and R. Schiavilla, Phys. Rev. C **51**, 38 (1995).
[24] H. de Vries, C. W. de Jager, and C. de Vries, At. Data Nucl. Data Tables **36**, 496 (1987).
[25] A. Fabrocini, F. Arias de Saavedra, G. Có, and P. Folgarait, Phys. Rev. C **57**, 1668 (1998).
[26] A. Fabrocini, F. Arias de Saavedra and G. Có, Phys. Rev. C **61**, 044302 (2000).
[27] G. Có, A. Fabrocini, S. Fantoni, and E. Lagaris, Nucl. Phys. A **549**, 439 (1992).
[28] G. Có, A. Fabrocini, and S. Fantoni, Nucl. Phys. A **568**, 73 (1994).
[29] F. Arias de Saavedra, G. Có, A. Fabrocini, and S. Fantoni, Nucl. Phys. A **605**, 359 (1996).
[30] F. Arias de Saavedra, G. Có, and A. Fabrocini, Phys. Rev. C **63**, 064308 (2001).
[31] F. Arias de Saavedra, G. Có, and M. M. Renis, Phys. Rev. C **55**, 673 (1997).
[32] H. Kümmel, K. H. Lührmann, and J. G. Zabolitzky, Phys. Rep. **36**, 1 (1978).
[33] L. Coraggio, N. Itaco, A. Covello, A. Gargano, and T. T. S. Kuo, Phys. Rev. C **68**, 034320 (2003).
[34] L. Coraggio, A. Covello, A. Gargano, N. Itaco, T. T. S. Kuo, and R. Machleidt, Phys. Rev. C **71**, 014307 (2005).
[35] R. Roth, T. Neff, H. Hergert, and H. Feldmeier, Nucl. Phys. A **745**, 3 (2004).
[36] C. Barbieri, N. Paar, R. Roth, and P. Papakonstantinou, arXiv:nucl-th/0608011.

[37] G. Hagen, D. J. Dean, M. Hjorth-Jensen, T. Papenbrock, and A. Schwenk, Phys. Rev. C **76**, 044305 (2007).
[38] P. Navrátil, J. P. Vary, and B. R. Barrett, Phys. Rev. Lett. **84**, 5728 (2000).
[39] P. Navrátil, J. P. Vary, and B. R. Barrett, Phys. Rev. C **62**, 054311 (2000).
[40] P. Navrátil and W. E. Ormand, Phys. Rev. C **68**, 034305 (2003).
[41] J. Carlson, Phys. Rev. C **38**, 1879 (1988).
[42] S. C. Pieper, R. B. Wiringa, and V. R. Pandharipande, Phys. Rev. C **46**, 1741 (1992).
[43] B. S. Pudliner, V. R. Pandharipande, J. Carlson, S. C. Pieper, and R. B. Wiringa, Phys. Rev. C **56**, 1720 (1997).
[44] A. Kievsky, M. Viviani, and S. Rosati, Nucl. Phys. A **551**, 241 (1993).
[45] S. C. Pieper, R. B. Wiringa, and J. Carlson, Phys. Rev. C **70**, 054325 (2004).
[46] S. C. Pieper, K. Varga, and R. B. Wiringa, Phys. Rev. C **66**, 044310 (2002).
[47] S. C. Pieper and R. B. Wiringa, Annu. Rev. Nucl. Part. Sci. **51**, 53 (2001).
[48] S. C. Pieper, V. R. Pandharipande, R. B. Wiringa, and J. Carlson, Phys. Rev. C **64**, 014001 (2001).
[49] S. C. Pieper, Nucl. Phys. A **751**, 516 (2005).
[50] C. R. Chen, G. L. Payne, J. L. Friar, and B. F. Gibson, Phys. Rev. C **33**, 1740 (1986).
[51] A. Stadler, W. Glöckle, and P. U. Sauer, Phys. Rev. C **44**, 2319 (1991).
[52] A. M. Green, Rep. Prog. Phys. **39**, 1109 (1976).
[53] J. W. Clark, Prog. Part. Nucl. Phys. **2**, 89 (1979).
[54] V. R. Pandharipande and R. B. Wiringa, Rev. Mod. Phys. **51**, 821 (1979).
[55] B. Friedman and V. R. Pandharipande, Nucl. Phys. A **361**, 502 (1981).
[56] R. B. Wiringa, V. Fiks, and A. Fabrocini, Phys. Rev. C **38**, 1010 (1988).
[57] I. E. Lagaris and V. R. Pandharipande, Nucl. Phys. A **359**, 331 (1981).
[58] R. B. Wiringa, R. A. Smith, and T. L. Ainsworth, Phys. Rev. C **29**, 1207 (1984).
[59] K. E. Schmidt and V. R. Panharipande, Phys. Lett. B **87**, 11 (1979).
[60] A. Akmal, V. R. Pandharipande, and D. G. Ravenhall, Phys. Rev. C **58**, 1804 (1998).
[61] V. Somà and P. Bożek, Phys. Rev. C **78**, 054003 (2008).
[62] K. Hebeler, S. K. Bogner, R. J. Furnstahl, A. Nogga, and A. Schwenk, Phys. Rev. C **83**, 031301(R) (2011).
[63] J. Carlson, V. R. Pandharipande, and R. B. Wiringa, Nucl. Phys. A **401**, 59 (1983).
[64] D. R. Entem and R. Machleidt, Phys. Rev. C **68**, 041001 (2003).
[65] M. Modarres, T. Pourmirjafari, and H. R. Moshfegh, Nucl. Phys. A **819**, 27 (2009).
[66] M. Modarres and T. Pourmirjafari, Nucl. Phys. A **836**, 91 (2010).
[67] M. Modarres and T. Pourmirjafari, Nucl. Phys. A **848**, 92 (2010).
[68] M. Modarres, A. Tafrihi, and A. Hatami, Nucl. Phys. A **879**, 1 (2012).
[69] K. Tsukiyama, S. K. Bogner, and A. Schwenk, Phys. Rev. Lett. **106**, 222502 (2011).
[70] C. Barbieri and M. Hjorth-Jensen, Phys. Rev. C **79**, 064313 (2009).
[71] Shinichiro Fujii, Ryoji Okamoto, and Kenji Suzuki, Phys. Rev. C **69**, 034328 (2004).
[72] S. Fujii, R. Okamoto, and K. Suzuki, Phys. Rev. Lett. **103**, 182501 (2009).
[73] G. Hagen, T. Papenbrock, D. J. Dean, and M. Hjorth-Jensen, Phys. Rev. Lett. **101**, 092502 (2008).
[74] G. Hagen, T. Papenbrock, D. J. Dean, and M. Hjorth-Jensen, Phys. Rev. C **82**, 034330 (2010).
[75] G. Hagen and H. Ah Nam, arXiv:1203.3765v1.
[76] J. M. Irvine, *Nuclear Structure Theory* (Pergamon Press, New York, 1972).
[77] A. de-Shalit and I. Talmi, *Nuclear Shell Theory* (Academic Press, New York, 1963).
[78] T. Brody and M. Moshinsky, *Tables of Transformation Brackets* (Mexico Instituto de Fisica, Mexico City, 1960).
[79] B. T. Smith, J. M. Boyle, J. J. Dongarra, B. S. Garbow, Y. Ikebe, V. C. Klema, and C. B. Moler, *Lecture Notes in Computer Science*, 2nd ed. (Springer-Verlag, Berlin, 1976), Vol. 6.